Hydrogen Storage in Several Metal-Phosphate Molecular Sieves

Jinxiang Dong, Guizhi Ban, Qiang Zhao, Lei Liu, and Jinping Li
Research Institute of Special Chemicals, Taiyuan University of Technology, Taiyuan, Shanxi 030024, P.R. China

DOI 10.1002/aic.11591
Published online October 9, 2008 in Wiley InterScience (www.interscience.wiley.com).

The hydrogen storage properties of metal-phosphate molecular sieves $AlPO_4$-5, $AlPO_4$-53, SAPO-34, $(NH_4)ZnPO_4$-HEX, and ZrPO-Py have been investigated at 77 K and 195 K and at pressures of 0–1.7 MPa. The hydrogen storage capacity is up to 1.0 wt % on $AlPO_4$-5, 1.30 wt % on $AlPO_4$-53, 1.42 wt % on SAPO-34, 0.68 wt % on $(NH_4)ZnPO_4$-HEX, and 0.72 wt % on ZrPO-Py at 77 K and 1.7 MPa. At 195 K and 1.7 MPa, the hydrogen storage capacity is 0.50 wt % on $AlPO_4$-5, 0.48 wt % on $AlPO_4$-53, 0.55 wt % on SAPO-34, 0.50 wt % on $(NH_4)ZnPO_4$-HEX, and 0.54 wt % on ZrPO-Py. The hydrogen storage capacities of samples increase with decreasing temperature.
 AIChE J, 54: 3017–3025, 2008
Keywords: hydrogen storage, metal-phosphate, molecular sieves, synthesis, low temperature

Introduction

Hydrogen energy is currently a topic of intensive research because of the ever-growing environmental concerns over the use of fossil fuels. Hydrogen storage is vital to the effective use of hydrogen energy, and up to now, several methods have been proposed for this. For example, physisorption, high-pressure tanks for gaseous hydrogen, cryogenic vessels for liquid hydrogen, and metal hydride storage systems are all under discussion.[1–4]

Recently, physisorption has attracted the most attention because the adsorption is reversible and thus the adsorbent can be recycled. Moreover, physisorption offers the possibility of high hydrogen storage capacity and rapid hydrogen desorption. As a result, many investigations have focused on encapsulated hydrogen molecules in microporous media at low temperature.[5–7] Molecular sieves, which are rich in abundant cage and channel structures and have high thermal stability,[8] offer great potential for encapsulation of nonpolar gases.

Metal-phosphate molecular sieves are an important family of microporous materials. They have been used in catalysis and adsorption.[9,10] However, there have only been a limited number of studies on their hydrogen storage. For example, the hydrogen storage capacity of H-SAPO-34 is reported as 1.09 wt % at 0.092 MPa and 77 K.[11] Forster et al.[12] reported that molecular sieves VSB-1 and VSB-5 (nickel phosphates) exhibit a capacity of H_2 sorption that is $\sim$ 10 cm^3/g and 60 cm^3/g, respectively, at 77 K and 600 Torr. They demonstrated that there were different sorption mechanisms in VSB-1 and VSB-5. VSB-1 shows the typical physisorption behavior of a nanoporous material, whereas VSB-5 appears to interact strongly with H_2 at low loadings and then continues to adsorb additional H_2 through weaker physisorption as the pressure is increased.

In this study, the authors investigated the hydrogen storage on metal-phosphate molecular sieves with different frameworks and elemental compositions. One investigated framework molecular sieve, SAPO-34, and four new samples were chosen. So five metal-phosphate molecular sieves are as follows: $AlPO_4$-5, $AlPO_4$-53, SAPO-34, (NH_4) $ZnPO_4$-HEX, and ZrPO-Py were synthesized in the hydrothermal and ionothermal systems. The as-synthesized samples were characterized by thermogravimetry (TG), X-ray diffraction (XRD), and scanning electron microscopy (SEM). The hydrogen storage properties of the samples were investigated systemically at 195 K and 77 K using a volumetric method with a P-C-T hydrogen storage device.

Correspondence concerning this article should be addressed to J. Li at dongjinxiangwork@hotmail.com.

Experimental

Chemicals

In the experiments, methylamine (MA), CH_3NH_2, 25%, Beijing Chemical Reagents Company), morpholine (C_4H_9NO, 99%, Beijing Chemical Reagents Company), tetraethylammonium hydroxide (TEAOH, $C_8H_{21}NO$, 25%, Shanghai Bangcheng Chemical Company.), phosphoric acid (H_3PO_4, 85%, The Third Company of Tianjin Chemical Reagents), zirconium oxychloride ($ZrOCl_2 \cdot 8H_2O$, 99%, Sinopharm Group Chemical Reagent Co.), pyridine (C_5H_5N, 99.5%, Sinopharm Group Chemical Reagent Co.), hydrogen fluoride (HF, 40%, Beijing Chemical Company), zinc acetate [$Zn(Ac)_2 \cdot 2H_2O$, 99% Beijing Chemical Company], urea [$CO(NH_2)_2$, 99%, Sinopharm Group Chemical Reagent Co.], choline chloride ($C_5H_{14}NClO$, 98%, Shanghai San'aisi Reagent Co.) were the chemical reagents. Aluminium hydroxide [$Al(OH)_3$, 98%, Shijiazhuang Wuyue Curatorial Company] and fumed silicon (SiO_2, 98%, Shenyang Chemical Co.) were the commercial products. They were purchased from commercial sources and used directly in all experiments. The distilled water was produced in our laboratory.

Synthesis of molecular sieve $AlPO_4$-5

First, distilled water and aluminium hydroxide were added to a Teflon-lined autoclave with stirring. Phosphoric acid was then added with stirring, then TEAOH with vigorous stirring until homogeneous. The autoclave was sealed and heated in an oven at 423 ± 3 K for 3 days for crystallization of the sample. After crystallization, the synthesized samples were washed with distilled water in a centrifuge until pH 7, then dried at 373 ± 3 K.

Synthesis of molecular sieve $AlPO_4$-53

The reactive gel was prepared by mixing an appropriate amount of distilled water, aluminium hydroxide, phosphoric acid, and methylamine solution with stirring in a Teflon-lined autoclave. The autoclave was sealed and put into an oven at 453 ± 3 K for 3 days for crystallization. The as-synthesized samples were washed with distilled water in a centrifuge until pH 7, then dried at 373 ± 3 K.

Synthesis of molecular sieve SAPO-34

The reactive gel was prepared by mixing an appropriate amount of distilled water, aluminium hydroxide, phosphoric acid, silicon dioxide, and morpholine with stirring in a Teflon-lined autoclave. The autoclave was sealed and put into an oven at 473 ± 3 K for 2 days for crystallization. The as-synthesized samples were washed with distilled water in a centrifuge until pH 7, then dried at 373 ± 3 K.

Synthesis of molecular sieve $(NH_4)ZnPO_4$-HEX

First, zinc acetate, eutectic salt (It was composed with the molar ration of urea/choline chloride 2/1), phosphoric acid, hydrogen fluoride, which were weighed accurately by molar composition, were put into a Teflon-lined autoclave in that order, then the autoclave was sealed and heated in an oven at 453 ± 3 K for 69 h for crystallization. After crystallization, the sample was cooled naturally in air. The synthesized sample was washed with distilled water, filtered, then dried at 293 K in air.

Synthesis of molecular sieve ZrPO-Py

For the synthesis method and conditions for ZrPO-Py, see Ref. 13. The molar ratios of the starting reactants used for a typical synthesis were $3HF/1ZrO_2/0.5P_2O_5/3Pyridine/100H_2O$. The charged autoclaves were then placed in an oven at 453 ± 3 K for 7 days. The crystalline products were filtered, washed with distilled water, and finally dried at 333 ± 2 K overnight.

Characterization

The crystallinity and phase purity of the molecular sieves were measured by powder X-ray diffraction (XRD) with a Rigaku D/Max 2500 X-ray diffractometer with Cu Kα1 radiation and operating at 40 kV and 100 mA. The scan range was from 5 to 40° (2θ) at 1°/min. Morphological data were acquired through SEM using a JEOL JSM-6700F scanning electron microscope operating at 15.0 kV. The samples were coated with gold to increase their conductivity before scanning. TG was carried out in air at a heating rate of 10 K/min using a Netzsch STA409C balance.

Hydrogen storage measurements

The purity of the hydrogen source was 99.99%, and a trap was used on the hydrogen gas inlet stream and reaction tube. Isothermal desorption curves were measured with the hydrogen storage device (Figure 1). After removing the guest molecules, about 1 g of sample was put into the reaction tube after precise weighing. The samples were heated up to a set temperature which depended on the stability of the molecular sieves and were kept at that temperature for 3 h under vacuum, then cooled to 77 K or 195 K. The temperature was kept constant and the pressure was decreased in equal pressure steps. Hydrogen storage results were expressed as weight percent (wt %) hydrogen in the material.

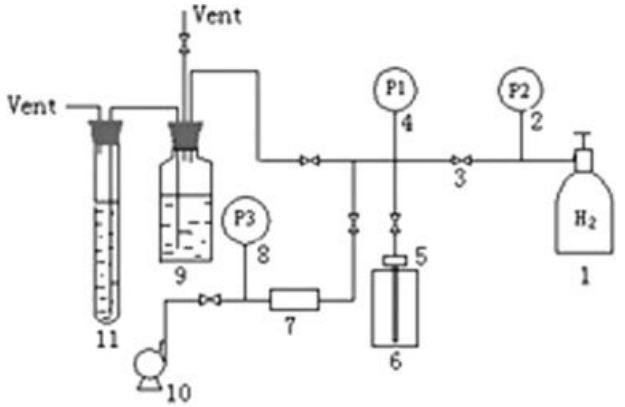

Figure 1. Apparatus for hydrogen storage measurement.

(1) hydrogen supply; (2) pressure gauge (0–16 MPa); (3) needle valve; (4) pressure gauge (0–10 MPa); (5) reaction tube; (6) constant temperature container; (7) buffer; (8) vacuum gauge; (9) gas bottle; (10) vacuum pump; (11) graduated flask.

Table 1. Effect of P_2O_5/Al_2O_3 on Synthesis of Molecular Sieve $AlPO_4$-5

Molar Composition of Reaction			Relative Crystallinity (%)	Phase
P_2O_5/Al_2O_3	R*/Al_2O_3	H_2O/Al_2O_3		
0.8	0.6	40	97	$AlPO_4$-5
1.0	0.6	40	100	$AlPO_4$-5
1.2	0.6	40	0	$AlPO_4$-H_4
1.5	0.6	40	0	$AlPO_4$-H_4

*R in this table is the tetraethylammonium hydroxide.

Table 2. Effect of P_2O_5/Al_2O_3 on Synthesis of Molecular Sieve $AlPO_4$-53

Molar Composition of Reaction			Relative Crystallinity (%)	Phase
P_2O_5/Al_2O_3	R*/Al_2O_3	H_2O/Al_2O_3		
0.8	1.25	40	67	$AlPO_4$-53
1.0	1.25	40	100	$AlPO_4$-53
1.2	1.25	40	95	$AlPO_4$-53
1.5	1.25	40	72	$AlPO_4$-53

*R in this table is the methylamine.

Table 3. Effect of P_2O_5/Al_2O_3 on Synthesis of Molecular Sieve SAPO-34

Molar Composition of Reaction				Relative Crystallinity (%)	Phase
P_2O_5/Al_2O_3	R*/Al_2O_3	SiO_2/Al_2O_3	H_2O/Al_2O_3		
0.5	2.1	1.08	66	66	SAPO-34
0.8	2.1	1.08	66	97	SAPO-34
1.06	2.1	1.08	66	100	SAPO-34
1.3	2.3	1.08	66	0	SAPO-5 +SAPO-11 +$AlPO_4$

*R in this table is the morpholine.

Results and Discussion

Synthesis of molecular sieve $AlPO_4$-5

Molecular sieve $AlPO_4$-5 was synthesized according to Ref. 14. The effects of synthesis conditions were investigated (Table 1). It was found that the ratio of P/Al is an important factor in the formation of molecular sieve $AlPO_4$-5 and significantly influences its crystallinity and phase purity. The results in Table 1 show that molecular sieve $AlPO_4$-5 may be prepared at P/Al = 0.8–1.0 and the sample with highest relative crystallinity was synthesized at P_2O_5/Al_2O_3 = 1, $TEAOH/Al_2O_3$ = 0.6, and H_2O/Al_2O_3 = 40 (molar ratio) by treating at 423 K for 3 days. Aluminium phosphate H_4 without micropores (JCPDS 48-35) is a phase with high P/Al ratio in reactive gel.[15]

Synthesis of molecular sieve $AlPO_4$-53

Molecular sieve $AlPO_4$-53 was synthesized according to the literature.[16] The effects of synthesis conditions were investigated (Table 2). It was found that the chemical composition range for synthesis of molecular sieve $AlPO_4$-53 was wide with P_2O_5/Al_2O_3 = 0.8–1.5 and the sample with the highest relative crystallinity was synthesized at P_2O_5/Al_2O_3 = 1.0, MA/Al_2O_3 = 1.25, and H_2O/Al_2O_3 = 40 (molar ratio) by treating at 453 K for 3 days.

Synthesis of molecular sieve SAPO-34

Molecular sieve SAPO-34 was synthesized according to Ref. 17. The effects of synthesis conditions were investigated (Table 3). It is found that the chemical composition range of synthesis molecular sieve SAPO-34 was wide with P/Al = 0.5–1.06 and the sample with the highest relative crystallinity was synthesized at P_2O_5/Al_2O_3 = 1.06, SiO_2/Al_2O_3 = 1.08, C_4H_9NO/Al_2O_3 = 2.1, and H_2O/Al_2O_3 = 66 (molar ratio) by treating at 473 K for 2 days. Three phases, SAPO-5,[14] SAPO-11,[18] and $AlPO_4$ (JCPDS 48-652),[19] were produced in high P/Al reactive gel.

Synthesis of molecular sieve $(NH_4)ZnPO_4$-HEX

Molecular sieve (NH_4) $ZnPO_4$-HEX was synthesized to discover new frameworks for molecular sieve ZnPO-n through the ionothermal method. Referring to the research of Professor Morris and coworkers[20] on molecular sieves $AlPO_4$-n, we investigated the possibility to synthesize molecular sieve ZnPO-n. The data in Table 4 showed that molecular sieve (NH_4) $ZnPO_4$-HEX, prepared in the hydrothermal system, may also be obtained in the ionothermal system. The crystals of molecular sieve (NH_4) $ZnPO_4$-HEX were prepared with a eutectic salt, urea, and choline chloride. The investigation of synthesis conditions showed that the molecular sieve (NH_4) $ZnPO_4$-HEX may be prepared at P/Zn = 1.67–7.5. In hydrogen storage experiments, the sample of molecular sieve $(NH_4)ZnPO_4$-HEX was synthesized from P/F/Zn/EU = 2.57:5.31:1:167 (molar ratio) by treating at 453 K for 69 h.

Thermoanalysis, phase, and morphology

To study the suitability of active experimental samples, the thermoanalysis technique was employed to measure the thermal stability and decomposition of organic molecules in the synthesized samples (Figure 2). XRD was used to measure the phase purity of the synthesized samples, and the phase transformation and framework collapse of calcined samples (Figure 3). SEM was used to observe the morphological changes before and after desorption of guest molecules (Figure 4).

Characterization of $AlPO_4$-5

The TG curve of molecular sieve $AlPO_4$-5 in Figure 2a shows that the material undergoes a slow continuous weight

Table 4. Effect of P/Zn on Synthesis of $(NH_4)ZnPO_4$-HEX

Molar Composition of Reaction			Phase
P/Zn	F/Zn	Eu*/Zn	
1.25	5.31	167	Amorphous
1.67	5.31	167	(NH_4) $ZnPO_4$
2.57	5.31	167	(NH_4) $ZnPO_4$
5.0	5.31	167	(NH_4) $ZnPO_4$
7.5	5.31	167	(NH_4) $ZnPO_4$

*Eu in this table is the urea/choline chloride = 2 (molar ration).

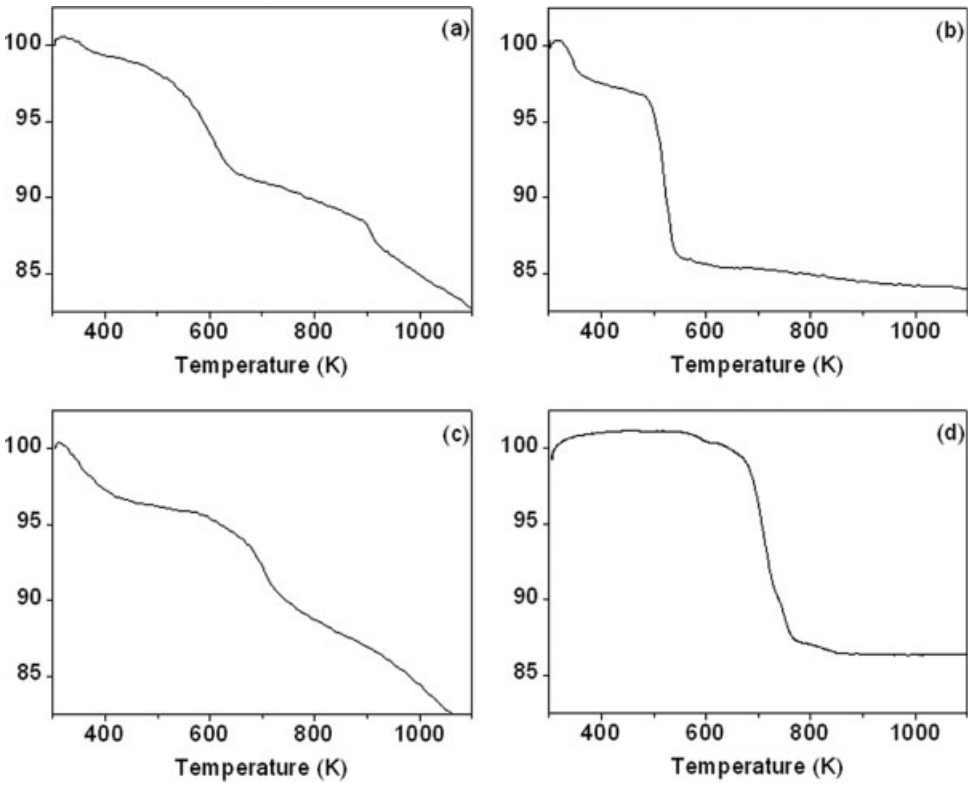

Figure 2. Thermograms of $AlPO_4$-5 (a), $AlPO_4$-53 (b), SAPO-34 (c), and $(NH_4)ZnPO_4$-HEX (d).

loss between RT and 1073 K. The low-temperature weight loss of 1.5% between room temperature and 473 K is assigned to the desorption of water from the framework. The weight loss of 7.32% between 473 K and 673 K is assigned to decomposition of TEAOH occluded inside the channels, while the weight loss of 4.51% in the range of 673–923 K is assigned to the desorption and decomposition of protonated amine which comes from the template agent TEAOH in the synthesis process, balancing the framework negative charge. The weight loss after 923 K may be caused by the collapse of the framework.

Figure 3a shows the XRD pattern of synthesized molecular sieve $AlPO_4$-5 compared with the standard XRD data for molecular sieve $AlPO_4$-5.[21] The peak positions and relative diffraction intensity are similar to the reported data and prove that molecular sieve $AlPO_4$-5 has been synthesized. Figure 3b shows the XRD pattern of molecular sieve $AlPO_4$-5 calcined at 773 K. Its peak positions and relative diffraction intensity are the same as the synthesized sample except that the relative intensities of the peaks at $2\theta = 12.89^\circ$ and 14.89° were interchanged. This shows that the sample is still molecular sieve $AlPO_4$-5 phase after removal of the guest molecules. Figure 3c shows the XRD of $AlPO_4$-5 calcined at 873 K for 6 h. Compared with the synthesized sample, the diffraction intensity of molecular sieve $AlPO_4$-5 had clearly decreased and this shows the framework collapse of $AlPO_4$-5 calcined at 873 K. So, in the experiments, the samples of molecular sieve $AlPO_4$-5 were calcined at 773 K for 6 h to remove the guest molecules (water and TEAOH) and produce the hydrogen storage samples.

Figure 4a shows the SEM of synthesized molecular sieve $AlPO_4$-5. It can be seen that $AlPO_4$-5 forms an aggregation of small plates. Figure 4b shows the SEM of molecular sieve $AlPO_4$-5 calcined at 773 K for 6 h and it can be seen that the aggregates of $AlPO_4$-5 have divided into small irregular particles when calcined at 773 K.

Characterization of $AlPO_4$-53

The TG curve of $AlPO_4$-53 in Figure 2b shows a small weight loss of 3.57% between RT and 473 K, which is attributed to the loss of some residual physisorbed water. A more significant weight loss of 10.93% occurred in the range of 473–873 K and reflects the loss of methylamine.

Figure 3d shows the XRD pattern of synthesized molecular sieve $AlPO_4$-53. By comparison with standard data for $AlPO_4$-53(A),[16] its diffraction peak positions and relative diffraction intensities were found to be the same as the standard data. So, the sample is molecular sieve $AlPO_4$-53(A). Figure 3e shows the XRD pattern of molecular sieve $AlPO_4$-53 calcined at 673 K for 6 h. The new phase, $AlPO_4$-53(B) in literature,[16] was formed at this temperature. By comparison with synthesized $AlPO_4$-53(A), some peak positions changed. This may be attributed to the removal of the guest molecules, which can explain the weight loss of methylamine in the range of 473–573 K. When comparing the XRD patterns of molecular sieve calcined at 773 K for 6 h (see Figure 3f), its peak positions and relative diffraction intensity are the same as the sample calcined at 673 K. In hydrogen storage experiments, the samples were calcined at 673 K for 6 h to remove

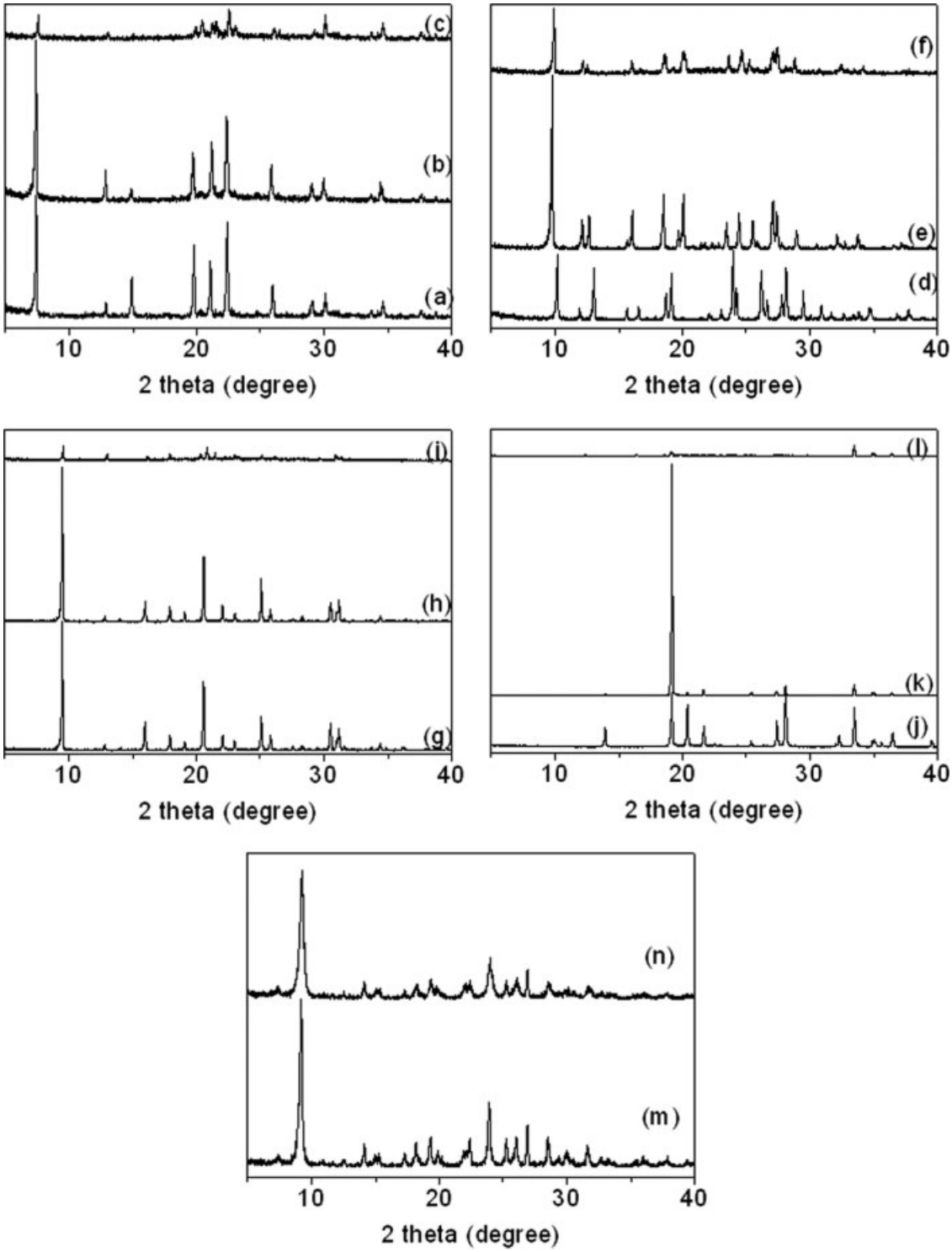

Figure 3. XRD patterns of $AlPO_4$-5, $AlPO_4$-53, SAPO-34, $(NH_4)ZnPO_4$-HEX, and ZrPO-Py.

(a) XRD of molecular sieve $AlPO_4$-5 synthesized sample. (b) XRD of molecular sieve $AlPO_4$-5 sample calcined at 773 K. (c) XRD of molecular sieve $AlPO_4$-5 sample calcined at 873 K. (d) XRD of molecular sieve $AlPO_4$-53 synthesized sample. (e) XRD of molecular sieve $AlPO_4$-53 sample calcined at 673 K. (f) XRD of molecular sieve $AlPO_4$-53 sample calcined at 773 K. (g) XRD of molecular sieve SAPO-34 synthesized sample. (h) XRD of molecular sieve SAPO-34 sample calcined at 823 K. (i) XRD of molecular sieve SAPO-34 sample calcined at 873 K. (j) XRD of molecular sieve (NH_4) $ZnPO_4$-HEX synthesized sample. (k) XRD of molecular sieve (NH_4) $ZnPO_4$-HEX sample calcined at 523 K. (l) XRD of molecular sieve (NH_4) $ZnPO_4$-HEX sample calcined at 573 K. (m) XRD of molecular sieve ZrPO-Py synthesized sample. (n) XRD of molecular sieve ZrPO-Py sample calcined at 673 K.

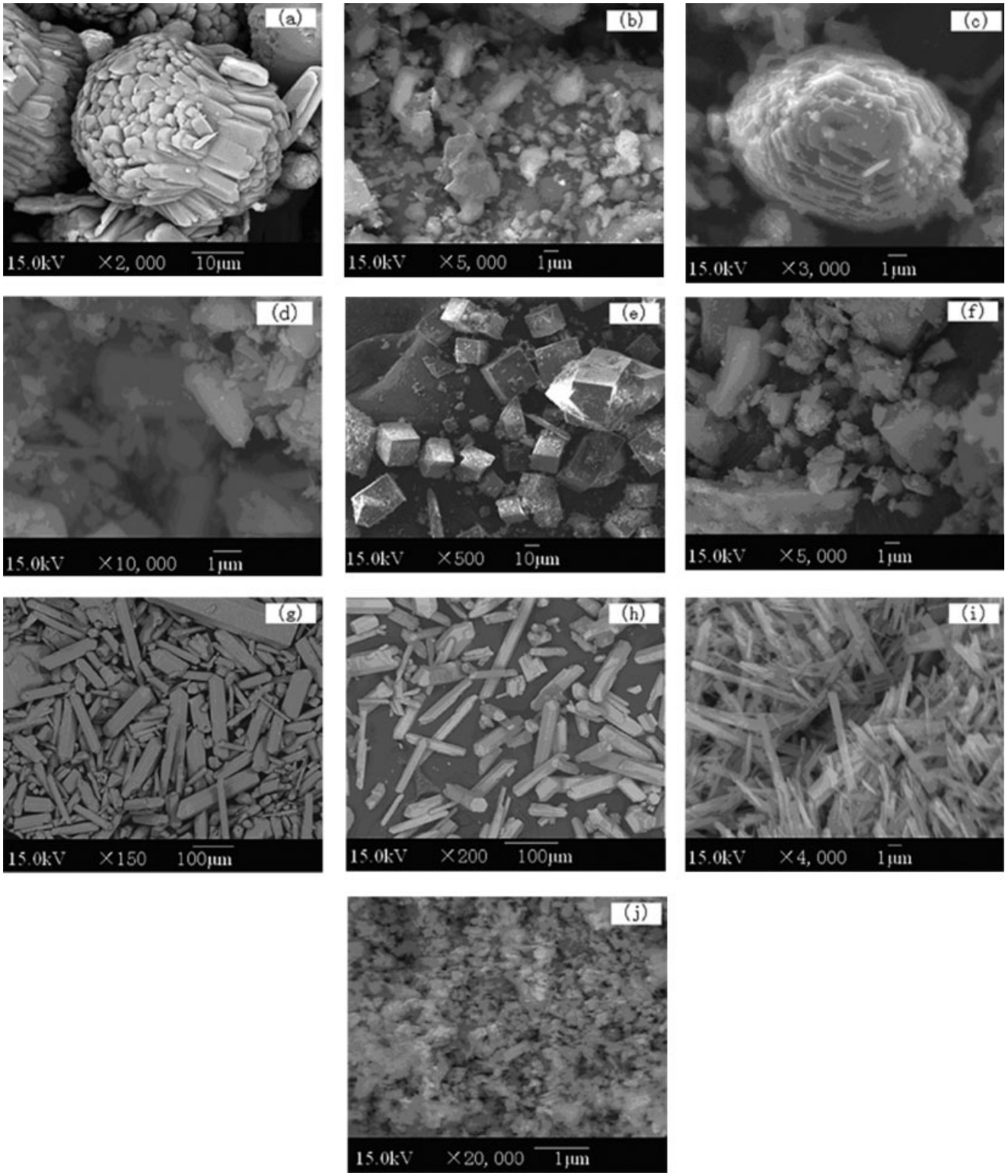

Figure 4. SEM of molecular sieves $AlPO_4$-5, $AlPO_4$-53, SAPO-34, $(NH_4)ZnPO_4$-HEX, and ZrPO-Py.

(a) SEM of molecular sieve $AlPO_4$-5 synthesized sample. (b) SEM of molecular sieve $AlPO_4$-5 sample calcined at 773 K. (c) SEM of molecular sieve $AlPO_4$-53 synthesized sample. (d) SEM of molecular sieve $AlPO_4$-53 sample calcined at 673 K. (e) SEM of molecular sieve SAPO-34 synthesized sample. (f) SEM of molecular sieve SAPO-34 sample calcined at 823 K. (g) SEM of molecular sieve (NH_4) $ZnPO_4$-HEX synthesized sample. (h) SEM of molecular sieve (NH_4) $ZnPO_4$-HEX sample calcined at 523 K. (i) SEM of molecular sieve ZrPO-Py synthesized sample. (j) SEM of molecular sieve ZrPO-Py sample calcined at 673 K.

the guest molecules (water and methylamine) to retain the framework and produce the hydrogen storage sample.

Figure 4c shows the SEM of synthesized molecular sieve $AlPO_4$-53. It shows that molecular sieves $AlPO_4$-53 are also aggregates of small plates. Figure 4d shows the SEM of molecular sieve $AlPO_4$-53 calcined at 673 K for 6 h and shows that the aggregates of small plates have divided into small irregular particles after calcining.

Characterization of SAPO-34

The TG curve of SAPO-34 in Figure 2c shows the same trend as for $AlPO_4$-5. The sample has a slow continuous weight loss between RT and 1073 K. The small weight loss of 4.12% below 473 K was assigned to water loss from the framework; weight loss of 6.99% was observed between 473 K and 723 K, which was attributed to the desorption and decomposition of morpholine; the more obvious weight loss between 723 K and 1073 K may arise from the removal of some hydroxyl in the framework.

Figure 3g shows the XRD pattern of synthesized molecular sieve SAPO-34. By comparison with standard data for SAPO-34,[22] its diffraction peak positions and relative diffraction intensities were found to be the same as the standard data and proved that the typical sample was SAPO-34. Figure 3h shows the XRD pattern of molecular sieve SAPO-34 calcined at 823 K. Its peak positions and relative diffraction intensity are the same as in the synthesized sample except that the relative intensity of the peak at $2\theta = 16.02^\circ$ was reduced, but this did not affect the phase of SAPO-34. This shows that the sample is still molecular sieve SAPO-34 phase after removing the guest molecules. Figure 3i shows that the relative diffraction intensity of molecular sieve SAPO-34 had clearly decreased after calcining at 873 K for 6 h. So, in experiments, the samples were calcined at 823 K for 6 h to remove guest molecules (water and morpholine) and obtain hydrogen storage samples.

Figure 4e shows the SEM of synthesized molecular sieve SAPO-34 and it can be seen that it has cuboidal crystals with size up to $25 \times 25 \times 25\ \mu m^3$. Figure 4f shows the SEM of molecular sieve SAPO-34 calcined at 823 K for 6 h and it can be seen that the cuboidal crystals have been destroyed during calcining and have divided into irregular particles.

Characterization of (NH_4) $ZnPO_4$-HEX

The TG curve of (NH_4) $ZnPO_4$-HEX is shown in Figure 2d. It is evident that there is no weight loss up to 573 K. Obvious weight loss of 10.09% was observed between 573 K and 773 K which is readily attributed to the remove of the guest molecules in the framework and the collapse of the framework.

Figure 3j shows the XRD pattern of synthesized molecular sieve (NH_4) $ZnPO_4$-HEX compared with the standard XRD data for that sieve.[23] The peak positions and relative diffraction intensity are similar to the reported data and prove that molecular sieve (NH_4) $ZnPO_4$-HEX has been synthesized. Figure 3k shows the XRD pattern of molecular sieve (NH_4) $ZnPO_4$-HEX calcined at 523 K. Its peak positions are the same as in the synthesized sample. The relative intensities of peaks at $2\theta = 13.93^\circ$ and 32.27° were reduced and the relative intensity of the peak at $2\theta = 19.13^\circ$ was increased significantly but the result showed that the sample was still molecular sieve (NH_4) $ZnPO_4$-HEX after calcining at 523 K for 6 h. Figure 3l shows the XRD of (NH_4) $ZnPO_4$-HEX calcined at 573 K for 6 h and it can be seen that collapse of the framework has started, which can easily explain the weight loss in the range 573–773 K. In hydrogen storage experiments, the samples were chose to be calcined at 523 K for 6 h in order to keep the integral framework and hydrogen storage samples were obtained.

Figure 4g shows the SEM of synthesized molecular sieve (NH_4) $ZnPO_4$-HEX. It can be seen that this sieve has hexagonal rod-like crystals up to a size of $130 \times 30 \times 30\ \mu m^3$. Figure 4h shows the SEM of molecular sieve (NH_4) $ZnPO_4$-HEX calcined at 523 K for 6 h. It shows the same crystalline morphology as in Figure 4g and indicates that this phase is not destroyed when calcining.

Characterization of ZrPO-Py

The thermal stability of molecular sieve ZrPO-Py was published in Ref. 13. Its thermal stability is lower than molecular sieves $AlPO_4$-5, $AlPO_4$-53, and SAPO-34.

The XRD pattern of ZrPO-Py in Figure 3m was also compared with Ref. 13 and the results showed that diffraction peak positions and relative diffraction intensities in the sample were the same as in the reference. After calcining at 673 K for 6 h (Figure 3n), the peak positions and relative intensity are the same as in the synthesized sample. This shows that the sample is still molecular sieve ZrPO-Py after calcining at 673 K for 6 h. When calcined at 723 K and 773 K for 6 h respectively, the intensities of the molecules of ZrPO-Py decrease obviously at 723 K. Phase transformation of the molecules of ZrPO-Py begin to take place at 773 K (see Ref. 13). So in experiments, molecular sieve ZrPO-Py was calcined at 673 K for 6 h to partly remove guest molecules (pyridine and water) as much as possible under the condition of integral framework and hydrogen storage samples were obtained.

Figure 4i shows the SEM of synthesized molecular sieve ZrPO-Py and elongate crystals with dimensions $9 \times 1 \times 0.7\ \mu m^3$ can be seen. Figure 4j shows the SEM of molecular sieve ZrPO-Py calcined at 673 K for 6 h and it can been seen that, after calcining, the crystals are now aggregates of small irregular particles.

Hydrogen storage properties

In this study, the isothermal hydrogen uptake of metal-phosphate molecular sieves was activated at different temperatures under the condition of integral framework, which was measured by the P-C-T method at low temperature. The hydrogen storage capacities of these five metal-phosphate molecular sieves have not been reported at 195 K. According to Figure 5, the hydrogen storage capacity is 0.5 wt % on $AlPO_4$-5, 0.48 wt % on $AlPO_4$-53, 0.55 wt % on SAPO-34, 0.50 wt % on (NH_4) $ZnPO_4$-HEX, and 0.54 wt % on ZrPO-Py at 1.7 MPa and 195 K. The hydrogen storage values of all of the samples are around 0.5 wt %. Analysis of hydrogen adsorption isotherms according to the Langmuir equation indicates that physisorption is the mechanism involved. This

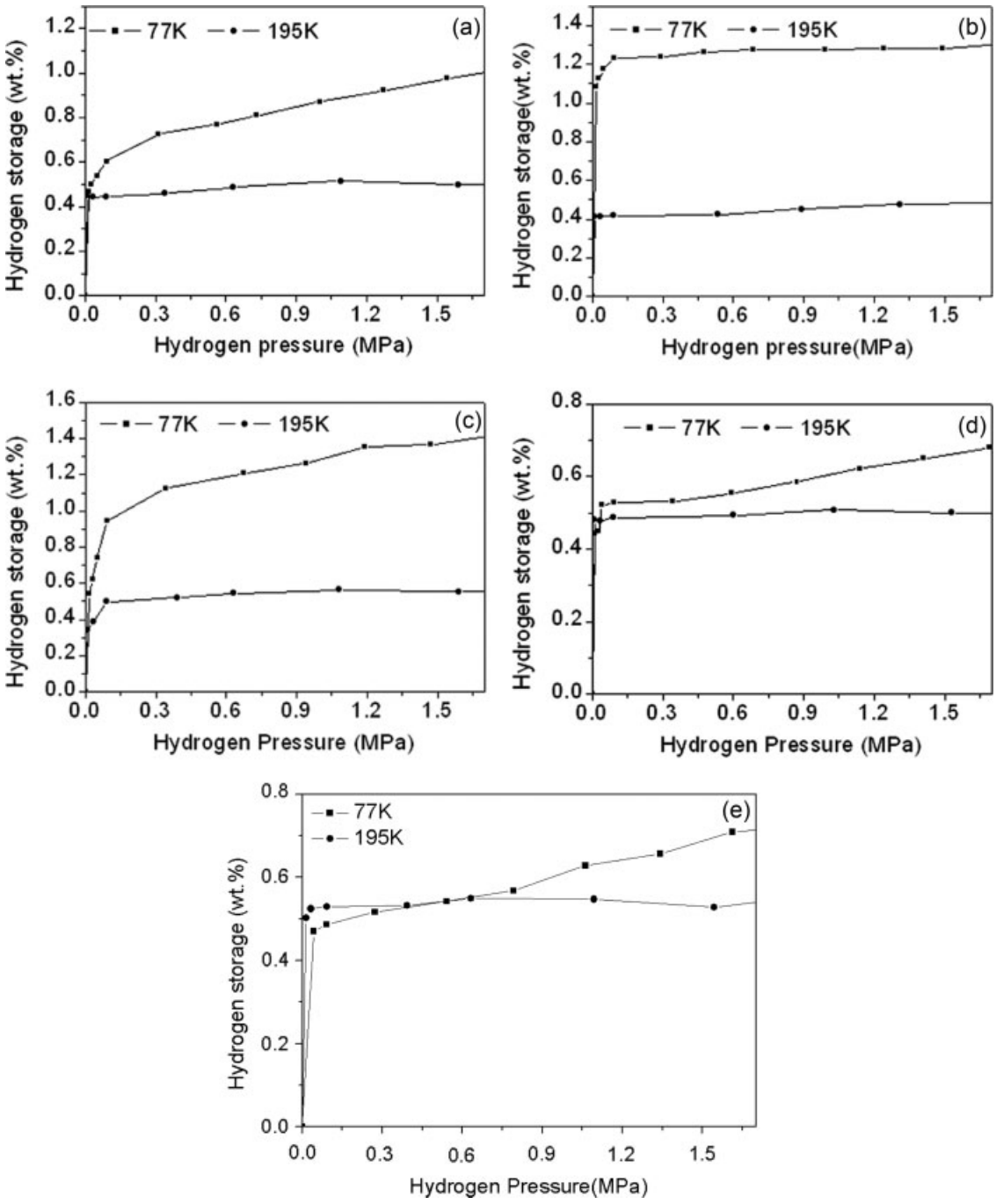

Figure 5. Hydrogen storage capacity of $AlPO_4$-5 (a), $AlPO_4$-53 (b), SAPO-34 (c), (NH_4) $ZnPO_4$-HEX (d), and ZrPO-Py (e) at 195 K and 77 K.

means that these five metal-phosphate molecular sieves all have definite hydrogen storage capacities at 195 K.

Next, the hydrogen storage capacities of the sieves were measured at 77 K. According to Figure 5, the hydrogen uptake capacity is 1.0 wt % on $AlPO_4$-5, 1.30 wt % on $AlPO_4$-53, 1.42 wt % on SAPO-34, 0.68 wt % on (NH_4) $ZnPO_4$-HEX, and 0.72 wt % on ZrPO-Py at 1.7 MPa and 77 K. The reported hydrogen storage capacities of VSB-1 and VSB-5 are 0.11 wt % and 0.57 wt % , respectively, at 0.079 MPa and 77 K. Compared with these, the hydrogen storage values of $AlPO_4$-53 and SAPO-34 are 1.1 wt % and 0.88 wt %, respectively, under the same conditions, which is much higher than the values of VSB-1 and VSB-5, and the value of $AlPO_4$-5 is 0.58 wt %, which is very similar to that of VSB-5 under the same conditions. The values of (NH_4) $ZnPO_4$-HEX and ZrPO-Py are 0.52 wt % and 0.48 wt %, respectively, which are slightly lower than that of VSB-5 and much higher than that of VSB-1 under the same conditions.

According to reported data, the molecular sieve H-SAPO-34 had a hydrogen storage capacity of 1.09 wt % at 0.092 MPa and 77 K. In our experiment, the hydrogen storage value of SAPO-34 is 0.94 wt % under the same conditions.

Certainly, the hydrogen storage capacities of different SAPO-34 molecular sieve samples are similar.

Compared with the date at 195 K, the hydrogen storage capacities at 77 K clearly increased. The hydrogen storage capacities of molecular sieves $AlPO_4$-5, $AlPO_4$-53, and SAPO-34 clearly increased with the decrease in temperature but the trends decreased with increasing pressure. The hydrogen storage capacities of (NH_4) $ZnPO_4$-HEX and ZrPO-Py increased slightly with the decrease in temperature but the capacity had an increasing trend with increasing hydrogen pressure. On the one hand, the difference in the two trends may be caused by the different activation centers in the frameworks. On the other hand, it may be the guest molecular were still in (NH_4) $ZnPO_4$-HEX at 523 K and the guest molecular were not removed completely ZrPO-Py at 673 K.

Conclusions

In this article, the thermal stabilities of metal-phosphate molecular sieves with different frameworks and elemental compositions were investigated. Suitable temperatures were found for removing guest molecules in the different molecular sieves. Experimental data show that the hydrogen storage capacities of the five metal-phosphate molecular sieves are around 0.5 wt % at 195 K and 1.7 MPa and the capacities increase with decreasing temperature. The capacities of molecular sieves $AlPO_4$-5, $AlPO_4$-53, and SAPO-34 increase more than (NH_4) $ZnPO_4$-HEX and ZrPO-Py.

Acknowledgments

The authors gratefully acknowledge financial support from the National Natural Science Foundation of China (No. 20573077, 50672063), the Natural Science Foundation of Shanxi Province (2006011021) and the Special Funds for Major State Technological Research 863 Project (No. 2007AA05Z153).

Literature Cited

1. Nijkamp MG, Raaymakers JEMJ, van Dillen AJ, Jong KP. Hydrogen storage using physisorption-materials demands. *Appl Phys A*. 2001;72:619–923.
2. Peschka W. Operating characteristics of a LH_2-fuelled automotive vehicle and of a semi-automatic LH_2-refuelling station. *Int J Hydrogen Energy*. 1982;7:661–669.
3. Amankwah KAG, Noh JS, Schwarz JA. Hydrogen storage on superactivated carbon at refrigeration temperatures. *Int J Hydrogen Energy*. 1989;14:437–447.
4. Miyaoka H, Ichikawa T, Isobe S, Fujii H. Hydrogen storage properties of nano-structural carbon and metal hydrides composites. *Phys B Condens Matter*. 2006;38:51–52.
5. Weitkamp J, Fritz M, Ernst S. Zeolites as media for hydrogen storage. *Int J Hydrogen Energy*. 1995;20:967–970.
6. Lee SM, Park KS, Choi YC, Park YS, Bok JM, Bae DJ, Nahm KS, Choi YG, Yu SC, Kim N, Frauenheim T, Lee YH. Hydrogen adsorption and storage in carbon nanotubes. *Synthetic Met*. 2000; 113:209–216.
7. Li YW, Yang RT. Significantly enhanced hydrogen storage in metal-organic frameworks via spillover. *J Am Chem Soc*. 2006;128: 726–727.
8. Langmi HW, Book D, Walton A, Johnson SR, Al-Mamouri MM, Speight JD, Edwards PP, Harris IR, Anderson PA. Hydrogen storage in ion-exchanged zeolites. *J Alloy Comp*. 2005;404–406: 637–642.
9. Hartmann M, Kevan L. Substitution of transition metal ions into aluminophosphates and silicoaluminophosphates: characterization and relation to catalysis. *Res Chem Intermed*. 2002;28:625–695.
10. Schuth F. Non-siliceous mesostructured and mesoporous materials. *Chem Mater*. 2001;13:3184–3195.
11. Zecchna A, Bordiga S, Vitillo JG, Ricchiardi G, Lamberti C, Spoto G, Bjrgen M, Lillerud KP. Liquid hydrogen in protonic chabazite. *J Am Chem Soc*. 2005;127:6361–6366.
12. Forster PM, Eckert J, Chang JS, Park SE, Ferey G, Cheetham AK. Hydrogen storage in nanoporous nickel (II) phosphates. *J Am Chem Soc*. 2003;125:1309–1312.
13. Dong JX, Liu L, Li JP, Li Y, Baerlocher C, McCusker LB. Synthersis, characterization and crystal structure of an open framework zirconium phosphate. *Microporous Mesoporous Mater*. 2007;104:185–191.
14. Wilson ST, Lok B, Flanigen E. Crystalline metallophosphate compositions. US Patent 4,310,440, 1982.
15. Duncan B, Stocker M, Gwinup D, Szostak R, Vinje K. Template-free synthesis of the aluminophates H1 through H4. *Soc Chim Fr*. 1992;129:98–110.
16. Kirchner RM, Grosse-Kunstleve RW, Pluth JJ, Wilson ST, Broach RW, Smith JV. The structures of as-synthesized $AlPO_4$-53(A), dehydrated $AlPO_4$-53(B),and $AlPO_4$-53(C)'a new phase determined by the FOCUS method. *Microporous Mesoporous Mater*. 2000;39:319–332.
17. Prakash AM, Unnikrishnan S. Synthesis of SAPO-34: high silicon incorporation in the presence of morpholine as template. *J Chem Soc Faraday Trans*. 1994;90:2291–2296.
18. Treacy MMJ, Higgins JB. *Collection of Simulated XRD Powder Patterns for Zeolites*. Amsterdam: Elsevier, 2001:9–10.
19. Debnath R, Chaudhuri J. Surface-bound titania-induced selective growth and stabilization of tridymite aluminum phosphate. *J Solid State Chem*. 1992;97:163–168.
20. Cooper ER, Andrews CD, Wheatley PS, Webb PB, Wormald P, Morris RE. Ionic liquids and eutectic mixtures as solvent and template in synthesis of zeolite analogues. *Nature*. 2004;430:1012–1016.
21. Treacy MMJ, Higgins JB. *Collection of Simulated XRD Powder Patterns for Zeolites*. Amsterdam: Elsevier, 2001:19–20.
22. Treacy MMJ, Higgins JB. *Collection of Simulated XRD Powder Patterns for Zeolites*. Amsterdam: Elsevier, 2001:87–88.
23. Harrison WTA, Alexandre NS, Phillips ML. Hexagonal ammonium zinc phosphate, (NH_4)$ZnPO_4$ at 10 K. *Acta Cryst C*. 2001;57:508–509.

Manuscript received Nov. 22, 2007, and revision received Jun. 10, 2008.